

Spectroscopic Study of Anisotropic Excitons in Single Crystal Hexacene

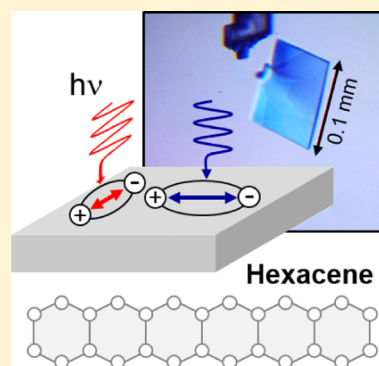
Alexey Chernikov,^{*,†} Omer Yaffe,[†] Bharat Kumar,[‡] Yu Zhong,[‡] Colin Nuckolls,[‡] and Tony F. Heinz^{*,†}

[†]Departments of Physics and Electrical Engineering, Columbia University, New York, New York 10027, United States

[‡]Department of Chemistry, Columbia University, New York, New York 10027, United States

S Supporting Information

ABSTRACT: The linear optical response of hexacene single crystals over a spectral range of 1.3–1.9 eV was studied using polarization-resolved reflectance spectroscopy at cryogenic temperatures. We observe strong polarization anisotropy for all optical transitions. Pronounced deviations from the single-molecule, solution-phase spectra are present, with a measured Davydov splitting of 180 meV, indicating strong intermolecular coupling. The energies and oscillator strengths of the relevant optical transitions and polarization-dependent absorption coefficients are extracted from quantitative analysis of the data.



SECTION: Spectroscopy, Photochemistry, and Excited States

Linear acenes, that is, naphthalene, anthracene, tetracene, and pentacene, form a unique family of organic semiconductors. These materials readily form large ($>100 \mu\text{m}^2$) single crystals that exhibit a “herring-bone” packing motif in which aromatic edge-to-face interactions dominate.¹ During the last few decades, this family has been the subject of many experimental and theoretical studies,² especially motivated by potential applications in flexible, low-cost optoelectronic devices.^{3–5} The strength of the intermolecular interactions in linear acene crystals is now understood to increase steadily with the length of the acene molecule.⁶ This increased interaction is correlated with two major trends: an increase in charge carrier mobility⁷ and an increase in the extent to which the molecular electronic structure is perturbed by intermolecular coupling effects.^{6,8,9} The latter manifests itself directly in the optical spectra of the materials. Single crystals of smaller acenes preserve the characteristic absorption features of the individual molecules in solution, with transitions of Frenkel excitons featuring well-resolved vibronic sidebands. The optical response of the pentacene crystals, however, already shows marked deviations from the molecular picture, indicating the pronounced influence of intermolecular interactions.^{6,8,10}

In addition, increased intermolecular coupling is accompanied by a delocalization of the excitonic wave function, which is distributed among several neighboring molecules and can also lead to an increased charge-transfer (CT) character of the low-energy excitons.^{8,9,11,12} Such CT states are considered to be crucial for multiexciton effects such as singlet fission, an energy conversion process where an excited singlet state converts into two long-lived triplet states.^{9,12–18} Correlation has been

established between the degree of CT character and the so-called Davydov splitting (DS)¹⁹ of the low-lying excitons observed in polarization-resolved optical absorption spectra.⁶ Thus, experimental characterization of the intrinsic optical properties of organic crystals also facilitates rational design of advanced optoelectronic devices. Naturally, the steady increase of the intermolecular coupling from naphthalene to pentacene crystals provides a strong impetus for a systematic study of even larger linear acenes. Such studies have been inhibited by the lack of suitable synthetic methods. Recently, however, effective synthesis and crystallization methods for hexacene have been reported.⁷ In a previous work, we made use of this method to investigate the rate of singlet fission in polycrystalline hexacene films and the room-temperature optical response of hexacene single crystals.²⁰

Here, we study the linear optical response of hexacene single crystals by polarization-resolved reflectance spectroscopy at cryogenic temperatures. From quantitative analysis of the data, we extract the energies and oscillator strengths of the relevant, bright optical transitions and polarization-dependent absorption coefficients. The optical response of the crystalline hexacene is found to deviate significantly from the corresponding single-molecule solution-phase spectrum (measured in Si oil to avoid oxidation),²¹ indicating the presence of strong intermolecular interactions.

Received: August 11, 2014

Accepted: October 6, 2014

Published: October 6, 2014

Hexacene single crystals with an average thickness of several microns and lateral areas of 20–50 μm^2 were grown on a fused silica substrate using a recently reported synthesis and growth procedure.⁷ Micrographs of typical crystals are presented in the Supporting Information. Previous single crystal X-ray diffraction measurements have established that such crystals adopt a triclinic structure with a nearly rectangular in-plane unit-cell lying parallel to the substrate.⁷ Optical reflection measurements were performed at normal incidence, with samples held in a cryostat at a temperature of 77 K. We used a tungsten quartz halogen lamp as a broadband radiation source, with the incident light linearly polarized by a rotatable absorptive polarization filter. The reflected radiation was spectrally dispersed in a grating spectrometer and detected by a liquid-nitrogen-cooled CCD. Measurements were performed only on the thickest crystals (see micrographs in Supporting Information). These crystals were opaque and could be treated as semi-infinite in extent in the analysis below. To obtain absolute reflectance spectra for each polarization angle, we normalized the reflection from the sample by that from the fused silica substrate.

The measured reflectance spectra of the hexacene crystal are presented in Figure 1a for polarization angles between 0° and

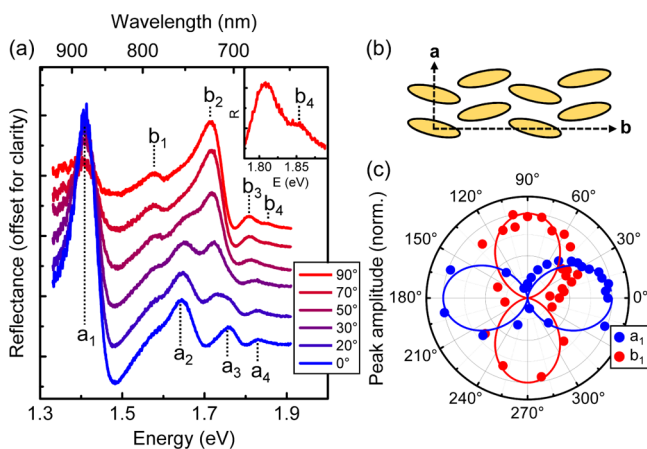


Figure 1. (a) Linearly polarized reflectance spectra of a hexacene single crystal at $T = 77$ K for polarization angles between 0° and 90°. The resonances excited with light polarized along the a axis (0°) and b axis (90°) of the crystal are denoted by a_1, \dots, a_4 and b_1, \dots, b_4 , respectively. The spectral region around the b_4 resonance in the 90° spectrum is presented in the inset. (b) Schematic representation of the hexacene crystal structure perpendicular to the growth direction with the symmetry axes denoted by “ a ” and “ b ”. (c) Polar plot of the normalized peak intensities of the lowest-lying exciton states (a_1, b_1) as a function of polarization angle. For comparison, the solid lines show \sin^2 functions.

90°. The two angles are typically assigned to be roughly aligned along the a and b symmetry axes of the crystal, schematically shown in Figure 1b. A manifold of resonances is observed with a strong dependence on the polarization angle. The optical transitions are labeled by a_1, \dots, a_4 and b_1, \dots, b_4 according to the respective polarization conditions. The resonances a_1 and b_1 are identified as the bright low-energy excitons measured at room-temperature in the previous study,²⁰ exhibiting a DS of their respective peak energies.¹⁹ The similarity of the optical spectra at room- and low-temperature indicates that there is no structural phase transition during the cooling process. A polar plot of the normalized amplitude of the two lowest-energy states (a_1, b_1) and the next two higher-lying states (a_2, b_2) is

presented in Figure 1). The \sin^2 curves shown in the same plot illustrate the pronounced polarization anisotropy of the respective transitions with about 90° between the a and b resonances. The amplitudes of the a - and b -related peaks nearly vanish in the spectra with the opposite polarization, with residual intensities attributed to a small angular tilt of the out-of-plane crystal axis or inhomogeneities.

To extract the energy and the oscillator strengths of the spectrally overlapping resonances in the reflectance spectra, we apply a quantitative analysis scheme based on a standard multi-Lorentzian parametrization²² of the complex dielectric function $\epsilon(E)$ with photon energy E and for the two polarizations along the principal optical axis

$$\epsilon(E) = \epsilon_b + \sum_k \frac{f_k}{E_{0,k}^2 - E^2 - i\gamma_k E} \quad (1)$$

with $E_{0,k}^2$, γ_k and f_k denoting the peak energy, spectral broadening and the oscillator strength of the k th transition, respectively. The background constant is represented by ϵ_b . The real and imaginary parts ϵ_1 and ϵ_2 of the dielectric function $\epsilon(E)$ are related to the complex refractive index ($n + i\kappa$) via

$$n(E) = \left[\frac{1}{2}(\epsilon_1 + \sqrt{\epsilon_1^2 + \epsilon_2^2}) \right]^{1/2} \quad (2)$$

$$\kappa(E) = \left[\frac{1}{2}(-\epsilon_1 + \sqrt{\epsilon_1^2 + \epsilon_2^2}) \right]^{1/2} \quad (3)$$

The reflectance spectrum for a semi-infinite bulk crystal at the normal incidence is then obtained from n and κ using

$$R(E) = \frac{[n - 1]^2 + \kappa^2}{[n + 1]^2 + \kappa^2} \quad (4)$$

The peak parameters in $\epsilon(E)$ for the a_1, \dots, a_4 and b_1, \dots, b_4 transitions are adjusted to ensure a fit of the multi-Lorentzian model to the measured reflectance spectra.

Two different dielectric functions are obtained for the a - and b -polarized cases, illustrating the anisotropy of the dielectric tensor in the acene crystals.^{23,24} In general, this analysis procedure is justified when the chosen polarization angles are close to or equivalent to the principal optical axis of the dielectric tensor. In the present case the substrate plane corresponds to the ab plane of the hexacene crystals and the latter is almost rectangular ($\gamma \approx 90^\circ$),^{7,20} that is, the crystal structure is nearly orthorhombic. For pentacene, the principal axes a and b indeed closely correspond to the orthogonal in-plane directions x and y ,¹⁰ justifying the assignment of the 0° and 90° polarization angles as being close to both principal optical and crystallographic axes.

The results of the above procedure are presented in Figure 2a, b, and c for the a -polarized (0°), unpolarized, and b -polarized (90°) spectra along with the measured data. The unpolarized spectrum is obtained by averaging the a - and b -polarized reflectance. The agreement of the results from the multi-Lorentzian analysis with the experimental data allows for a meaningful extraction of the peak parameters and related observables, such as the absorption coefficients $\alpha(E) = \kappa(E)(2E/\hbar c)$.²² The latter are presented in Figure 2d, e, and f for the three polarization conditions. The overall magnitude of the absorption coefficients is 10^4 – 10^5 cm^{-1} . This absorptivity is roughly comparable to that of the lower acenes, for example, to values extracted for tetracene crystals from the data in ref 23.

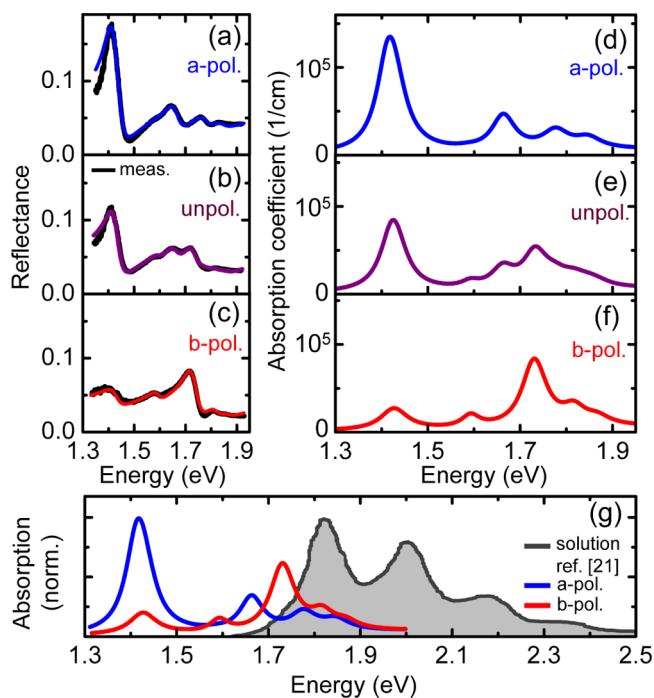


Figure 2. Measured and simulated reflectance spectra for *a*-polarized (a), unpolarized, (b) and *b*-polarized (c) light. (d), (e), and (f): Corresponding absorption coefficients extracted from the simulation. (g) The room-temperature spectrum of solution-phase hexacene from ref 21 is compared to the measured single crystal data.

For direct comparison of the overall spectral shape of the absorption, the normalized room-temperature spectrum of solution-phase hexacene from ref 21, is presented in Figure 2g together with the *a*- and *b*-polarized single crystal data. The lowest-energy peak in the spectrum of crystalline hexacene is red-shifted by 0.4 eV, as expected when going from solution to crystal, however the overall peak structure additionally exhibits pronounced deviations from the solution-phase data.

From the two lowest states, we extract a DS of 180 (± 10) meV, comparable to the room-temperature result of 160 meV.²⁰ In general, the origin of the splitting lies in the presence of two translationally inequivalent molecules in the unit cell of the crystal¹⁹ and the overall magnitude has been found to correlate with the degree of intermolecular CT character in the lowest-energy excitation, for the family of acenes.⁶ Therefore, the measured value in hexacene, which is considerably larger than the DS in pentacene of 100–130 meV,^{10,25,26} indicates a further increase in the CT contribution to the excitonic wave function.

The oscillator strengths of the optical transitions are presented in Figure 3 at the respective peak energies of the a_1, \dots, a_4 and b_1, \dots, b_4 resonances. The absolute values are comparable to the results from the analysis of the room-temperature data.²⁰ Neither the *a*-polarized nor *b*-polarized transitions have a form that resembles the vibronic progression of the isolated acene molecules, that is, roughly equidistant spacing between the peaks and decreasing peak areas for higher energies, as observed in anthracene²⁷ and tetracene²³ crystals as well as solution-phase hexacene.²¹ Instead, we observe a more complex peak structure, with anisotropy of the optical resonances and a nontrivial distribution of the oscillator strengths, more similar to what is seen in pentacene crystals.¹⁰ Such a response can be related to the underlying electronic

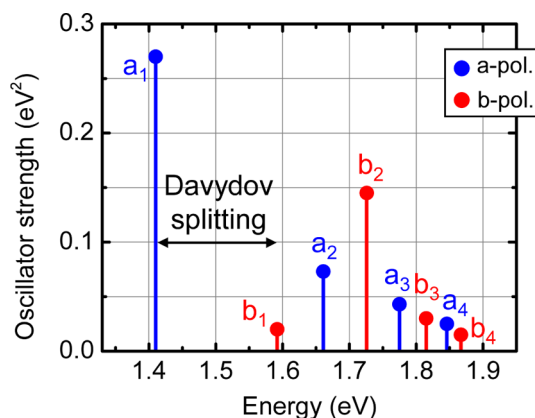


Figure 3. Energies and relative oscillator strengths of the *a*-polarized and *b*-polarized transitions in hexacene. The oscillator strengths are given in units of (eV^2). The Davydov splitting of 180 meV is indicated.

band-structure, which exhibits a pronounced dispersion due to the intermolecular coupling, as in theoretical calculations for pentacene crystals.^{8,9,12} Furthermore, as the authors of ref 6 pointed out, carrier–phonon coupling decreases with the length of the acene molecule as a result of the increasingly delocalized character of the excitations. Therefore, the vibronic replicas of the excitonic transitions should be significantly suppressed in hexacene crystals, in addition to the potential modifications of the phonon structure by intermolecular interactions.

In conclusion, we have studied the linear optical response of hexacene single crystals by polarization-resolved reflectance spectroscopy at cryogenic temperatures. Strongly anisotropic optical transitions are identified and quantitatively analyzed using a multi-Lorentzian modeling of the dielectric function. From this analysis, we extract the energies and oscillator strengths of the optical transitions, as well as the polarization-dependent absorption spectra. The overall optical response suggests a pronounced dispersion in the underlying single-particle (electronic) band structure, due to increased intermolecular interactions. In particular, the large DS of 180 meV in hexacene implies a significant CT character of the low-lying excitations, which is relevant for intermolecular phenomena such as singlet fission, exciton dissociation, and exciton–exciton scattering. Finally, the carefully characterized linear optical properties of this newest member of the acene family should allow for further development and benchmarking of computational methods as well as for the evaluation of hexacene’s potential in optoelectronic devices.

■ ASSOCIATED CONTENT

Supporting Information

Optical micrographs of hexacene crystals on a quartz substrate: 2.5 \times optical micrograph of hexacene crystals, 10 \times optical micrograph of hexacene crystals. This material is available free of charge via the Internet at <http://pubs.acs.org>.

■ AUTHOR INFORMATION

Corresponding Authors

*E-mail: aac2183@columbia.edu

*E-mail: tony.heinz@columbia.edu

Notes

The authors declare no competing financial interest.

■ ACKNOWLEDGMENTS

Overall project coordination, sample growth and optical characterization were supported as part of the Center for Redefining Photovoltaic Efficiency Through Molecular-Scale Control, an Energy Frontier Research Center funded by the U.S. Department of Energy (DOE), Office of Science, Office of Basic Energy Sciences under Award DE-SC0001085. O.Y. is a Marie Curie IOF fellow. A.C. gratefully acknowledges funding from the Alexander von Humboldt Foundation within the Feodor Lynen Fellowship program. The authors would like to thank Timothy Berkelbach (Columbia University) and Kolja Kolata (Philipps Universität Marburg) for helpful discussions.

■ REFERENCES

- (1) Suzuki, M.; Yokoyama, T.; Ito, M. Polarized Raman Spectra of Naphthalene and Anthracene Single Crystals. *Spectrochim. Acta, Part A* **1968**, *24*, 1091–1107.
- (2) Anthony, J. E. Functionalized Acenes and Heteroacenes for Organic Electronics. *Chem. Rev.* **2006**, *106*, 5028–5048.
- (3) Forrest, S. R. The Path to Ubiquitous and Low-Cost Organic Electronic Appliances on Plastic. *Nature* **2004**, *428*, 911–918.
- (4) Coropceanu, V.; Cornil, J.; da Silva Filho, D. A.; Olivier, Y.; Silbey, R.; Brédas, J.-L. Charge Transport in Organic Semiconductors. *Chem. Rev.* **2007**, *107*, 926–952.
- (5) Podzorov, V. Organic Single Crystals: Addressing the Fundamentals of Organic Electronics. *MRS Bull.* **2013**, *38*, 15–24.
- (6) Yamagata, H.; Norton, J.; Hontz, E.; Olivier, Y.; Beljonne, D.; Brédas, J. L.; Silbey, R. J.; Spano, F. C. The Nature of Singlet Excitons in Oligoacene Molecular Crystals. *J. Chem. Phys.* **2011**, *134*, 204703.
- (7) Watanabe, M.; Chang, Y. J.; Liu, S.-W.; Chao, T.-H.; Goto, K.; Islam, M. M.; Yuan, C.-H.; Tao, Y.-T.; Shinmyozu, T.; Chow, T. J. The Synthesis, Crystal Structure and Charge-Transport Properties of Hexacene. *Nat. Chem.* **2012**, *4*, 574–578.
- (8) Tiago, M.; Northrup, J.; Louie, S. Ab Initio Calculation of the Electronic and Optical Properties of Solid Pentacene. *Phys. Rev. B* **2003**, *67*, 115212.
- (9) Sharifzadeh, S.; Darancet, P.; Kronik, L.; Neaton, J. B. Low-Energy Charge-Transfer Excitons in Organic Solids from First-Principles: the Case of Pentacene. *J. Phys. Chem. Lett.* **2013**, *4*, 2197–2201.
- (10) Faltermeier, D.; Gompf, B.; Dressel, M.; Tripathi, A.; Pflaum, J. Optical Properties of Pentacene Thin Films and Single Crystals. *Phys. Rev. B* **2006**, *74*, 125416.
- (11) Sebastian, L.; Weiser, G.; Bässler, H. Charge Transfer Transitions in Solid Tetracene and Pentacene Studied by Electroabsorption. *Chem. Phys.* **1981**, *61*, 125–135.
- (12) Berkelbach, T. C.; Hybertsen, M. S.; Reichman, D. R. Microscopic Theory of Singlet Exciton Fission. III. Crystalline Pentacene. *J. Chem. Phys.* **2014**, *141*, 074705.
- (13) Smith, M. B.; Michl, J. Recent Advances in Singlet Fission. *Annu. Rev. Phys. Chem.* **2013**, *64*, 361–386.
- (14) Congreve, D. N.; Lee, J.; Thompson, N. J.; Hontz, E.; Yost, S. R.; Reuswig, P. D.; Bahlke, M. E.; Reineke, S.; Van Voorhis, T.; Baldo, M. A. External Quantum Efficiency above 100% in a Singlet-Exciton-Fission-Based Organic Photovoltaic Cell. *Science* **2013**, *340*, 334–337.
- (15) Berkelbach, T. C.; Hybertsen, M. S.; Reichman, D. R. Microscopic Theory of Singlet Exciton Fission. II. Application to Pentacene Dimers and the Role of Superexchange. *J. Chem. Phys.* **2013**, *138*, 114103.
- (16) Chan, W.-L.; Berkelbach, T. C.; Provorse, M. R.; Monahan, N. R.; Tritsch, J. R.; Hybertsen, M. S.; Reichman, D. R.; Gao, J.; Zhu, X.-Y. The Quantum Coherent Mechanism for Singlet Fission: Experiment and Theory. *Acc. Chem. Res.* **2013**, *46*, 1321–1329.
- (17) Yost, S. R.; Lee, J.; Wilson, M. W. B.; Wu, T.; McMahan, D. P.; Parkhurst, R. R.; Thompson, N. J.; Congreve, D. N.; Rao, A.; Johnson, K.; et al. A Transferable Model for Singlet-Fission Kinetics. *Nat. Chem.* **2014**, *6*, 492–497.
- (18) Kolata, K.; Breuer, T.; Witte, G.; Chatterjee, S. Molecular Packing Determines Singlet Exciton Fission in Organic Semiconductors. *ACS Nano* **2014**, *8*, 7377–7383.
- (19) Davydov, A. S. The Theory of Molecular Excitons. *Phys.-Usp.* **1964**, *7*, 145–178.
- (20) Busby, E.; Berkelbach, T. C.; Kumar, B.; Chernikov, A.; Zhong, Y.; Hlaing, H.; Zhu, X.-Y.; Heinz, T. F.; Hybertsen, M. S.; Sfeir, M. Y.; et al. Multiphonon Relaxation Slows Singlet Fission in Crystalline Hexacene. *J. Am. Chem. Soc.* **2014**, *136*, 10654–10660.
- (21) Angliker, H.; Rommel, E.; Wirz, J. Electronic Spectra of Hexacene in Solution (Ground State. Triplet State. Dication and Dianion). *Chem. Phys. Lett.* **1982**, *87*, 208–212.
- (22) Klingshirn, C. *Semiconductor Optics*, 3rd ed.; Springer: Berlin/Heidelberg/New York, 2007.
- (23) Tavazzi, S.; Raimondo, L.; Silvestri, L.; Spearman, P.; Camposeo, A.; Polo, M.; Pisignano, D. Dielectric Tensor of Tetracene Single Crystals: The Effect of Anisotropy on Polarized Absorption and Emission Spectra. *J. Chem. Phys.* **2008**, *128*, 154709.
- (24) Dressel, M.; Gompf, B.; Faltermeier, D.; Tripathi, A. K.; Pflaum, J.; Schubert, M. Kramers–Kronig-Consistent Optical Functions of Anisotropic Crystals: Generalized Spectroscopic Ellipsometry on Pentacene. *Opt. Exp.* **2008**, *16*, 19770–19778.
- (25) Prikhotko, A. F.; Tsikora, L. I. Spectral Investigations of Pentacene. *Opt. Spectrosc.* **1968**, *25*, 242–246.
- (26) Helzel, J.; Jankowski, S.; El Helou, M.; Witte, G.; Heimbrodt, W. Temperature Dependent Optical Properties of Pentacene Films on Zinc Oxide. *Appl. Phys. Lett.* **2011**, *99*, 211102.
- (27) Clark, L. B.; Philpott, M. R. Anisotropy of the Singlet Transitions of Crystalline Anthracene. *J. Chem. Phys.* **1970**, *53*, 3790.